

Thermoelectric Detection of Spherical Tin Inclusions in Copper by Magnetic Sensing

Hector Carreon, Prof. Peter B. Nagy, and Prof. Adnan H. Nayfeh
Department of Aerospace Engineering and Engineering Mechanics
University of Cincinnati, U.S.A.

I. INTRODUCTION

It was recently demonstrated by Hinken and Tavrin that self-referencing thermoelectric measurements can be done in an entirely noncontact way by using high-sensitivity magnetic detectors to sense the weak thermoelectric currents around inclusions and other types of inhomogeneities when the specimen to be tested is subjected to directional heating or cooling^{1,2}. A schematic diagram of the self-referencing thermoelectric method with noncontacting magnetic sensing is shown in **Figure1**.

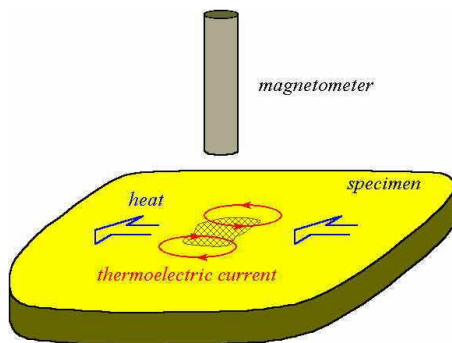


Figure 1:

External heating or cooling is applied to the specimen to produce a modest temperature gradient ($\approx 1\text{C}^\circ/\text{cm}$) in the region to be tested. As a result, different points of the boundary between the host material and the inclusion will be at different temperatures, therefore also at different thermoelectric potentials. These potential differences will produce opposite thermoelectric currents inside and outside the inclusion. The thermoelectric currents form two local loops that run in opposite directions on the two sides of the inclusion relative to the prevailing heat flux, which can be detected by scanning the specimen with a sensitive magnetometer, e.g., a fluxgate or a SQUID detector. Since the surrounding intact material serves as the “reference” electrode and there is no artificial interface between the host and the imperfect region to be detected, the detection sensitivity to variations in material properties could be very high and subtle effects such as local plastic deformation can also be detected³

The main goal of our current research effort is to help lay down the groundwork necessary to develop this new field of nondestructive testing and materials characterization based on noncontacting magnetic detection of thermoelectric currents. In a recent paper, Nagy and Nayfeh developed an analytical model to predict the magnetic field produced by thermoelectric currents around surface-breaking and subsurface spherical inclusions in a homogeneous host material under external thermal excitation⁴. The experimental results to be presented in this paper quantitatively verify those predictions through the examples of surface-breaking spherical tin inclusions of varying diameter in copper.

II. Experimental Method

Figure 2 shows a schematic diagram of the experimental arrangement.

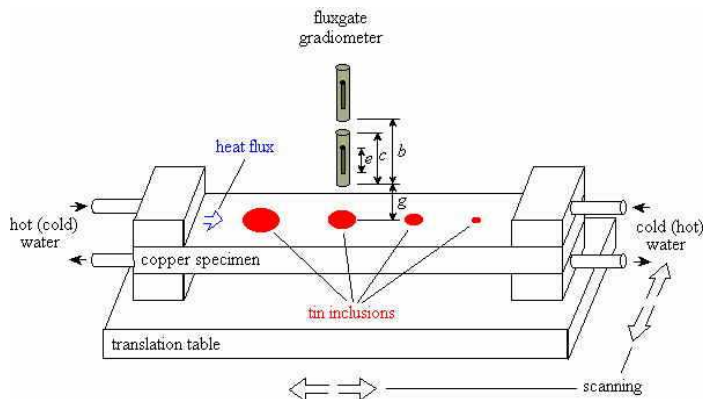


Figure 2:

We prepared a series of semi-spherical pure tin inclusions embedded in two pure copper bars of 12.7 mm 38.1 mm 500 mm dimensions. First, we prepared the semi-spherical holes by milling, then we heated the specimens to approximately 300 °C and filled the holes with molten tin, and finally milled the surface flat after the specimen has cooled down. The diameter of the inclusions varied from 2.38 mm to 12.7 mm and the center of each inclusion was at the level of the specimen's surface. The distance between inclusions was approximately 75 mm to avoid interference between their individual magnetic fields. Both ends of the copper bar were perforated by a series of holes and equipped with sealed heat exchangers to facilitate efficient heating and cooling and then mounted on a non-magnetic translation table for scanning. The ends of the copper bar were simultaneously heated and cooled by running water to temperatures of +10 °C and +40 °C, respectively. The actual temperature difference between the ends of the bar was monitored during the measurements by thermocouple thermometers and the temperature gradient was kept at 0.7 °C/cm, which is more than sufficient to produce detectable magnetic signals in high-conductivity materials like copper and tin.

The feasibility of self-referencing thermoelectric measurements by noncontact magnetic sensing crucially depends on the sensitivity of the magnetometer. Fortunately, as a result of recent technological advances in high-sensitivity magnetic sensors, state-of-the-art magnetometers, such as Giant Magneto-Resistive (GMR) detectors, Spin Dependent Tunneling (SDT) detectors, fluxgates and, especially, Superconductive QUantum Interference Device (SQUID) magnetometers, it has become feasible to achieve very high sensitivity levels that were not attainable before. **Figure 3** shows the typical noise spectra of various magnetic sensors currently available on the market.

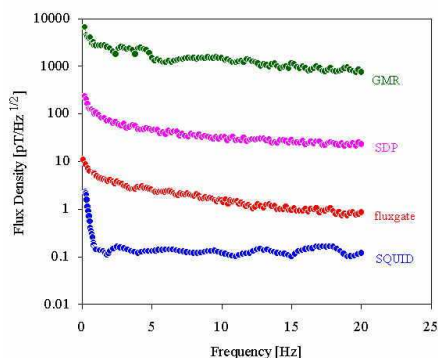


Figure 3:

Of course, the strength of the magnetic field to be detected greatly depends on the physical nature and dimensions of the imperfection, but for modest ($\approx 1\text{-}10^\circ\text{C/cm}$) temperature gradients the magnetic flux density is expected to be between 10 pT and 300 nT¹⁻⁴. The experimental results presented in this paper were obtained by a Bartington Instruments Mag-03 fluxgate that has a noise-limited detection threshold of 25 pT_{rms} over a bandwidth of 0.01-20 Hz. In comparison, the measured peak magnetic flux densities varied between 0.5 nT and 250 nT, i.e., the sensitivity of the fluxgate magnetometer was quite sufficient and the incoherent electrical noise produced by the sensor and the preamplifier had no significant effect on the accuracy of our measurements.

III. EXPERIMENTAL RESULTS

Figure 4 shows examples of the magnetic images obtained from two surface-breaking semi-spherical tin inclusions embedded in copper.

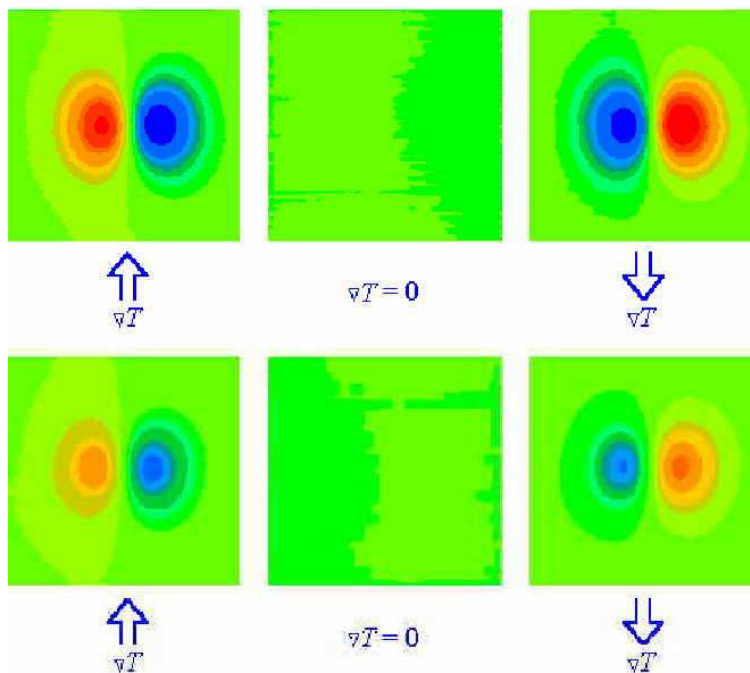


Figure 4:

These pictures were taken at $g = 2$ mm distance above the surface (see **Figure 2**). This apparent lift-off distance is the actual gap between the tip of the magnetometer probe and the specimen. However, the sensing element of the fluxgate is an $e = 15$ mm long ferromagnetic rod centered in a $c = 25$ mm long case. For simplicity, we can consider the fluxgate as a point sensor buried at a depth of approximately 12.5 mm below the tip of the case, i.e., the 2-mm apparent lift-off corresponds to a much larger 14.5-mm actual lift-off distance. The measured magnetic field distributions are very similar in shape to the previously derived analytical predictions⁴. As expected, the characteristic bi-polar lobes change sign when the direction of the temperature gradient in the specimen is reversed. These lobes get larger and the magnitude of the magnetic flux decreases when the lift-off distance is increased.

Figure 5 shows how the peak magnetic flux density changes with the apparent lift-off distance between 1 and 8 mm for six inclusions of different diameters between 2.38 mm and 12.7 mm. The solid lines represent our analytical predictions.⁴

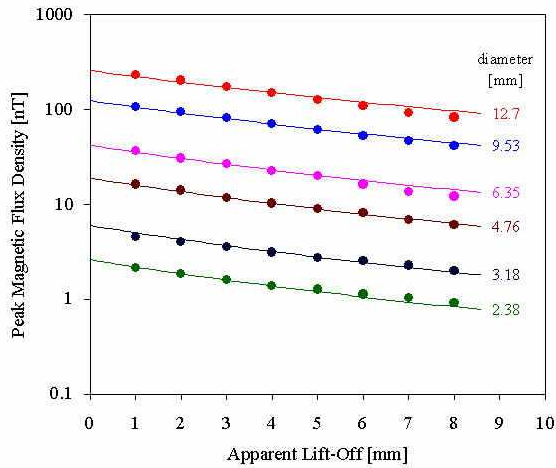


Figure 5:

For each inclusion diameter and lift-off distance, the theoretical values were calculated at two sensor positions corresponding to the primary and secondary fluxgates of the gradiometer and the values were subtracted. In most cases, subtraction of the magnetic field measured by the secondary sensor has a negligible effect on the result, but in the case of small inclusions and large lift-off distances the effect can be as high as 15-20%. The lift-off distance was corrected for the depth of the sensing element below the surface of the probe, but no other adjustments were made. Because of the decay of the magnetic field with increasing lift-off distance, the effective center of the sensing element is closer to the surface than its geometrical center. We tried to compensate the resulting inherent underestimation in the analytically predicted magnetic field by best fitting the numerical results to the experimental data using the unknown effective depth of the sensing element as the variable parameter. The least-mean-square fitting process yielded an optimal depth of 11.04 mm, slightly lower than the previously described rough approximation based on the geometrical center of the sensing element, as one would expect. With this reasonable adjustment, the standard deviation between the theoretical predictions and the experimental results is only 6.3% (based on the geometrical center of the sensor, i.e., without any adjustable parameter, the corresponding error is approximately 18%). The same results are plotted in a different way in **Figure 6** that compares the experimentally measured and theoretically predicted magnetic flux densities for all the different diameters and lift-off distances.

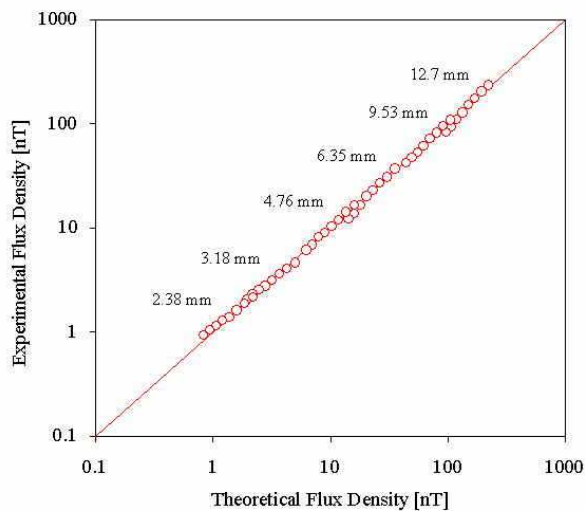


Figure 6.

Considering the rather crude approximations used in the theoretical model, the inherent uncertainties of the large number of independent material parameters involved in the phenomenon, and the potential experimental errors associated with the measurement, the

agreement over a range of more than two orders of magnitude is surprisingly good, possibly even fortuitous to some degree.

Another quantitative parameter that can be readily used to compare our analytical predictions and experimental observations is the half-width of the bi-polar magnetic signature, which was defined as half of the lateral separation between the positive and negative peaks. **Figure 7** shows our theoretical predictions (solid line) and experimental results (symbols) for the half-width of the magnetic signature as a function of lift-off.

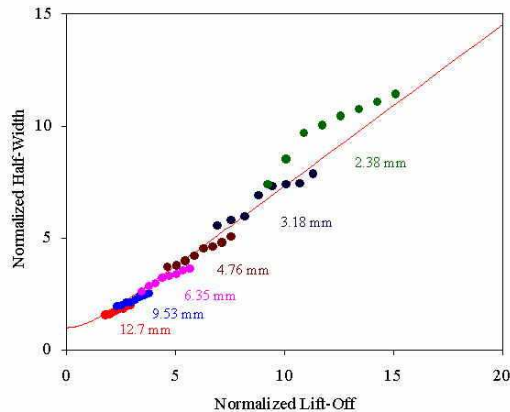


Figure 7:

There is a good agreement between the theoretical and experimental data except when the normalized lift-off distance exceeds 10. It should be mentioned that a large normalized lift-off results mainly from a small inclusion diameter, i.e., from the normalization process itself, rather than a large absolute lift-off. Since the peaks are not only smaller but also less sharp in the case of small inclusions, it is not surprising that the accuracy of the measured half-width also declines.

IV Conclusions

We conducted an experimental investigation of the magnetic field produced by thermoelectric currents around surface-breaking spherical tin inclusions in copper bars under external thermal excitation. The diameter of the inclusions and the lift-off distance varied from 2.38 to 12.7 mm and from 12 to 20 mm, respectively. We enforced a constant 0.7 °C/cm temperature gradient in the specimen. The resulting peak magnetic flux densities ranged from 1 to 250 nT and could be easily measured by a commercial fluxgate magnetometer. Our main goal was to verify the recently published theoretical predictions of Ref. 4. After appropriate normalization to facilitate such comparison, our experimental results were found to be in good quantitative agreement with the predictions of this model concerning both the absolute magnitude and the spatial distribution of the thermoelectric magnetic field. The results clearly indicate that inclusions and other types of imperfections in metals can not only be nondestructively detected by noncontacting magnetic measurements, but can also be quantitatively characterized using the previously developed analytical model.

REFERENCES

- ¹ J. H. Hinken and Y. Tavrín, "Thermoelectric SQUID method for the detection of segregations," in Review of Progress in Quantitative Nondestructive Evaluation, edited by D. O. Thompson and D. E. Chimenti, Vol. 19 (AIP, Melville, 2000) pp. 2085-2092.
- ² [J. H. Hinken and Y. Tavrín, "Detection of segregations in aero engine turbine discs with the thermoelectric SQUID method," 1999 ASNT Fall Conference \(Phoenix, Arizona, October 11-15, 1999\).](#)
- ³ Y. Tavrín, P. B. Nagy, and J. H. Hinken, "Detection of fatigue in aluminum with the thermoelectric SQUID method: A first attempt," Spot Beam, No. 26 (F.I.T. Messtechnik, Bad Salzdetfurth, 1999).
- ⁴ P. B. Nagy and A. H. Nayfeh, "The magnetic field of the thermoelectric currents produced by inclusions under thermal excitation," J. Appl. Phys. 87, 7481 (2000).